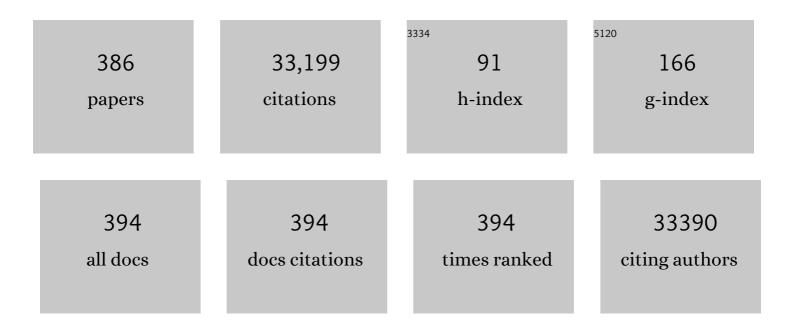
Weibo Cai

List of Publications by Year in descending order

Source: https://exaly.com/author-pdf/9403161/publications.pdf Version: 2024-02-01



#	Article	IF	CITATIONS
1	In vivo biodistribution and highly efficient tumour targeting of carbon nanotubes in mice. Nature Nanotechnology, 2007, 2, 47-52.	31.5	1,384
2	Nanozyme: new horizons for responsive biomedical applications. Chemical Society Reviews, 2019, 48, 3683-3704.	38.1	1,101
3	Circulation and long-term fate of functionalized, biocompatible single-walled carbon nanotubes in mice probed by Raman spectroscopy. Proceedings of the National Academy of Sciences of the United States of America, 2008, 105, 1410-1415.	7.1	1,037
4	Peptide-Labeled Near-Infrared Quantum Dots for Imaging Tumor Vasculature in Living Subjects. Nano Letters, 2006, 6, 669-676.	9.1	905
5	Applications of gold nanoparticles in cancer nanotechnology. Nanotechnology, Science and Applications, 2008, Volume 1, 17-32.	4.6	652
6	Nanoplatforms for Targeted Molecular Imaging in Living Subjects. Small, 2007, 3, 1840-1854.	10.0	558
7	Multimodality Molecular Imaging of Tumor Angiogenesis. Journal of Nuclear Medicine, 2008, 49, 113S-128S.	5.0	497
8	Biomedical Applications of Zinc Oxide Nanomaterials. Current Molecular Medicine, 2013, 13, 1633-1645.	1.3	495
9	Graphene: a versatile nanoplatform for biomedical applications. Nanoscale, 2012, 4, 3833.	5.6	478
10	Iron Oxide Decorated MoS ₂ Nanosheets with Double PEGylation for Chelator-Free Radiolabeling and Multimodal Imaging Guided Photothermal Therapy. ACS Nano, 2015, 9, 950-960.	14.6	460
11	cRGD-functionalized, DOX-conjugated, and 64Cu-labeled superparamagnetic iron oxide nanoparticles for targeted anticancer drug delivery and PET/MR imaging. Biomaterials, 2011, 32, 4151-4160.	11.4	410
12	Dual-Function Probe for PET and Near-Infrared Fluorescence Imaging of Tumor Vasculature. Journal of Nuclear Medicine, 2007, 48, 1862-1870.	5.0	400
13	NanoLuc: A Small Luciferase Is Brightening Up the Field of Bioluminescence. Bioconjugate Chemistry, 2016, 27, 1175-1187.	3.6	383
14	Non-invasive multimodal functional imaging of the intestine with frozen micellar naphthalocyanines. Nature Nanotechnology, 2014, 9, 631-638.	31.5	382
15	Synthesis and Biomedical Applications of Copper Sulfide Nanoparticles: From Sensors to Theranostics. Small, 2014, 10, 631-645.	10.0	380
16	Theranostic Liposomes with Hypoxia-Activated Prodrug to Effectively Destruct Hypoxic Tumors Post-Photodynamic Therapy. ACS Nano, 2017, 11, 927-937.	14.6	358
17	Engineering of inorganic nanoparticles as magnetic resonance imaging contrast agents. Chemical Society Reviews, 2017, 46, 7438-7468.	38.1	358
18	<i>In Vivo</i> Targeting and Imaging of Tumor Vasculature with Radiolabeled, Antibody-Conjugated Nanographene. ACS Nano, 2012, 6, 2361-2370.	14.6	318

#	Article	lF	CITATIONS
19	<i>In Vivo</i> Tumor Targeting and Image-Guided Drug Delivery with Antibody-Conjugated, Radiolabeled Mesoporous Silica Nanoparticles. ACS Nano, 2013, 7, 9027-9039.	14.6	314
20	DNA origami nanostructures can exhibit preferential renal uptake and alleviate acute kidney injury. Nature Biomedical Engineering, 2018, 2, 865-877.	22.5	297
21	Scintillating Nanoparticles as Energy Mediators for Enhanced Photodynamic Therapy. ACS Nano, 2016, 10, 3918-3935.	14.6	296
22	Preparation and functionalization of graphene nanocomposites for biomedical applications. Nature Protocols, 2013, 8, 2392-2403.	12.0	284
23	ImmunoPET: Concept, Design, and Applications. Chemical Reviews, 2020, 120, 3787-3851.	47.7	263
24	Effective weight control via an implanted self-powered vagus nerve stimulation device. Nature Communications, 2018, 9, 5349.	12.8	242
25	Theranostic Nanoparticles. Journal of Nuclear Medicine, 2014, 55, 1919-1922.	5.0	235
26	Molecular imaging and therapy of cancer with radiolabeled nanoparticles. Nano Today, 2009, 4, 399-413.	11.9	234
27	Effective Wound Healing Enabled by Discrete Alternative Electric Fields from Wearable Nanogenerators. ACS Nano, 2018, 12, 12533-12540.	14.6	234
28	Quantitative PET of EGFR expression in xenograft-bearing mice using 64Cu-labeled cetuximab, a chimeric anti-EGFR monoclonal antibody. European Journal of Nuclear Medicine and Molecular Imaging, 2007, 34, 850-858.	6.4	231
29	Preparation of peptide-conjugated quantum dots for tumor vasculature-targeted imaging. Nature Protocols, 2008, 3, 89-96.	12.0	228
30	Quantitative PET imaging of tumor integrin alphavbeta3 expression with 18F-FRGD2. Journal of Nuclear Medicine, 2006, 47, 113-21.	5.0	228
31	64Cu-Labeled Tetrameric and Octameric RGD Peptides for Small-Animal PET of Tumor ÂvÂ3 Integrin Expression. Journal of Nuclear Medicine, 2007, 48, 1162-1171.	5.0	227
32	FeSe ₂ â€Decorated Bi ₂ Se ₃ Nanosheets Fabricated via Cation Exchange for Chelatorâ€Free ⁶⁴ Cuâ€Labeling and Multimodal Imageâ€Guided Photothermalâ€Radiation Therapy. Advanced Functional Materials, 2016, 26, 2185-2197.	14.9	225
33	Multifunctional unimolecular micelles for cancer-targeted drug delivery and positron emission tomography imaging. Biomaterials, 2012, 33, 3071-3082.	11.4	224
34	HaloTag Technology: A Versatile Platform for Biomedical Applications. Bioconjugate Chemistry, 2015, 26, 975-986.	3.6	224
35	Anti-Angiogenic Cancer Therapy Based on Integrin αvβ3 Antagonism. Anti-Cancer Agents in Medicinal Chemistry, 2006, 6, 407-428.	1.7	222
36	Biodegradable and Renal Clearable Inorganic Nanoparticles. Advanced Science, 2016, 3, 1500223.	11.2	220

#	Article	IF	CITATIONS
37	Nanobody: The "Magic Bullet―for Molecular Imaging?. Theranostics, 2014, 4, 386-398.	10.0	219
38	PET of vascular endothelial growth factor receptor expression. Journal of Nuclear Medicine, 2006, 47, 2048-56.	5.0	217
39	CARM1 Methylates Chromatin Remodeling Factor BAF155 to Enhance Tumor Progression and Metastasis. Cancer Cell, 2014, 25, 21-36.	16.8	215
40	Cancer-Targeted Optical Imaging with Fluorescent Zinc Oxide Nanowires. Nano Letters, 2011, 11, 3744-3750.	9.1	199
41	Scavenging of reactive oxygen and nitrogen species with nanomaterials. Nano Research, 2018, 11, 4955-4984.	10.4	199
42	Imaging of Integrins as Biomarkers for Tumor Angiogenesis. Current Pharmaceutical Design, 2008, 14, 2943-2973.	1.9	198
43	InÂvivo targeting and positron emission tomography imaging of tumor vasculature with 66Ga-labeled nano-graphene. Biomaterials, 2012, 33, 4147-4156.	11.4	197
44	How molecular imaging is speeding up antiangiogenic drug development. Molecular Cancer Therapeutics, 2006, 5, 2624-2633.	4.1	192
45	In vitro and In vivo Characterization of 64Cu-Labeled AbegrinTM, a Humanized Monoclonal Antibody against Integrin αvβ3. Cancer Research, 2006, 66, 9673-9681.	0.9	192
46	Dual-modality optical and positron emission tomography imaging of vascular endothelial growth factor receptor on tumor vasculature using quantum dots. European Journal of Nuclear Medicine and Molecular Imaging, 2008, 35, 2235-2244.	6.4	189
47	Hexamodal Imaging with Porphyrinâ€Phospholipidâ€Coated Upconversion Nanoparticles. Advanced Materials, 2015, 27, 1785-1790.	21.0	189
48	Positron Emission Tomography Imaging Using Radiolabeled Inorganic Nanomaterials. Accounts of Chemical Research, 2015, 48, 286-294.	15.6	188
49	Molybdenum-based nanoclusters act as antioxidants and ameliorate acute kidney injury in mice. Nature Communications, 2018, 9, 5421.	12.8	184
50	Are quantum dots ready for inÂvivo imaging in human subjects?. Nanoscale Research Letters, 2007, 2, 265-281.	5.7	178
51	Engineering of Hollow Mesoporous Silica Nanoparticles for Remarkably Enhanced Tumor Active Targeting Efficacy. Scientific Reports, 2014, 4, 5080.	3.3	176
52	Comparison of the Superagonist Complex, ALT-803, to IL15 as Cancer Immunotherapeutics in Animal Models. Cancer Immunology Research, 2016, 4, 49-60.	3.4	176
53	Gold Nanorods Conjugated with Doxorubicin and cRGD for Combined Anticancer Drug Delivery and PET Imaging. Theranostics, 2012, 2, 757-768.	10.0	175
54	Activatable Hybrid Nanotheranostics for Tetramodal Imaging and Synergistic Photothermal/Photodynamic Therapy. Advanced Materials, 2018, 30, 1704367.	21.0	165

#	Article	IF	CITATIONS
55	Intrinsically Germaniumâ€69â€Labeled Iron Oxide Nanoparticles: Synthesis and Inâ€Vivo Dualâ€Modality PET/MR Imaging. Advanced Materials, 2014, 26, 5119-5123.	21.0	158
56	<i>In Vivo</i> Tumor Vasculature Targeting of CuS@MSN Based Theranostic Nanomedicine. ACS Nano, 2015, 9, 3926-3934.	14.6	155
57	Positron emission tomography and nanotechnology: A dynamic duo for cancer theranostics. Advanced Drug Delivery Reviews, 2017, 113, 157-176.	13.7	153
58	Preclinical Pharmacokinetics and Biodistribution Studies of ⁸⁹ Zr-Labeled Pembrolizumab. Journal of Nuclear Medicine, 2017, 58, 162-168.	5.0	152
59	Ceria Nanoparticles Meet Hepatic Ischemiaâ€Reperfusion Injury: The Perfect Imperfection. Advanced Materials, 2019, 31, e1902956.	21.0	150
60	Tumor vasculature targeting and imaging in living mice with reduced graphene oxide. Biomaterials, 2013, 34, 3002-3009.	11.4	149
61	Magnetic Targeting of Nanotheranostics Enhances Cerenkov Radiation-Induced Photodynamic Therapy. Journal of the American Chemical Society, 2018, 140, 14971-14979.	13.7	148
62	Biocompatibility and in vivo operation of implantable mesoporous PVDF-based nanogenerators. Nano Energy, 2016, 27, 275-281.	16.0	141
63	Molecular imaging with single-walled carbon nanotubes. Nano Today, 2009, 4, 252-261.	11.9	139
64	PET Tracers Based on Zirconium-89. Current Radiopharmaceuticals, 2011, 4, 131-139.	0.8	137
65	Cerenkov Radiation Induced Photodynamic Therapy Using Chlorin e6-Loaded Hollow Mesoporous Silica Nanoparticles. ACS Applied Materials & Interfaces, 2016, 8, 26630-26637.	8.0	136
66	<i>In Vivo</i> Integrity and Biological Fate of Chelator-Free Zirconium-89-Labeled Mesoporous Silica Nanoparticles. ACS Nano, 2015, 9, 7950-7959.	14.6	135
67	Bioresponsive Polyoxometalate Cluster for Redox-Activated Photoacoustic Imaging-Guided Photothermal Cancer Therapy. Nano Letters, 2017, 17, 3282-3289.	9.1	135
68	Bacteria-like mesoporous silica-coated gold nanorods for positron emission tomography and photoacoustic imaging-guided chemo-photothermal combined therapy. Biomaterials, 2018, 165, 56-65.	11.4	134
69	Wafer-scale heterostructured piezoelectric bio-organic thin films. Science, 2021, 373, 337-342.	12.6	129
70	A thiol-reactive 18F-labeling agent, N-[2-(4-18F-fluorobenzamido)ethyl]maleimide, and synthesis of RGD peptide-based tracer for PET imaging of alpha v beta 3 integrin expression. Journal of Nuclear Medicine, 2006, 47, 1172-80.	5.0	124
71	microPET of Tumor Integrin ÂvÂ3 Expression Using 18F-Labeled PEGylated Tetrameric RGD Peptide (18F-FPRGD4). Journal of Nuclear Medicine, 2007, 48, 1536-1544.	5.0	120
72	Chelatorâ€Free Synthesis of a Dualâ€Modality PET/MRI Agent. Angewandte Chemie - International Edition, 2013, 52, 13319-13323.	13.8	120

#	Article	IF	CITATIONS
73	18F-labeled mini-PEG spacered RGD dimer (18F-FPRGD2): synthesis and microPET imaging of αvβ3 integrin expression. European Journal of Nuclear Medicine and Molecular Imaging, 2007, 34, 1823-1831.	6.4	119
74	VEGF ₁₂₁ -Conjugated Mesoporous Silica Nanoparticle: A Tumor Targeted Drug Delivery System. ACS Applied Materials & Interfaces, 2014, 6, 21677-21685.	8.0	118
75	18F-labeled bombesin analogs for targeting GRP receptor-expressing prostate cancer. Journal of Nuclear Medicine, 2006, 47, 492-501.	5.0	118
76	Big Potential from Small Agents: Nanoparticles for Imaging-Based Companion Diagnostics. ACS Nano, 2018, 12, 2106-2121.	14.6	117
77	Surface Engineering of Graphene-Based Nanomaterials for Biomedical Applications. Bioconjugate Chemistry, 2014, 25, 1609-1619.	3.6	116
78	A new PET tracer specific for vascular endothelial growth factor receptor 2. European Journal of Nuclear Medicine and Molecular Imaging, 2007, 34, 2001-2010.	6.4	114
79	Renalâ€Clearable PEGylated Porphyrin Nanoparticles for Imageâ€Guided Photodynamic Cancer Therapy. Advanced Functional Materials, 2017, 27, 1702928.	14.9	113
80	A Melaninâ€Based Natural Antioxidant Defense Nanosystem for Theranostic Application in Acute Kidney Injury. Advanced Functional Materials, 2019, 29, 1904833.	14.9	111
81	Multimodality imaging of the HER-kinase axis in cancer. European Journal of Nuclear Medicine and Molecular Imaging, 2008, 35, 186-208.	6.4	109
82	Harnessing the Power of Nanotechnology for Enhanced Radiation Therapy. ACS Nano, 2017, 11, 5233-5237.	14.6	109
83	Seleniumâ€Đoped Carbon Quantum Dots Act as Broadâ€Spectrum Antioxidants for Acute Kidney Injury Management. Advanced Science, 2020, 7, 2000420.	11.2	109
84	Intrinsically Radiolabeled Nanoparticles: An Emerging Paradigm. Small, 2014, 10, 3825-3830.	10.0	106
85	Imaging with Raman Spectroscopy. Current Pharmaceutical Biotechnology, 2010, 11, 654-661.	1.6	104
86	Tumor-Targeted Drug Delivery with Aptamers. Current Medicinal Chemistry, 2011, 18, 4185-4194.	2.4	104
87	Near-Infrared Fluorescence Imaging of Tumor Integrin αvβ3 Expression with Cy7-Labeled RGD Multimers. Molecular Imaging and Biology, 2006, 8, 226-236.	2.6	102
88	Imaging of VEGF Receptor in a Rat Myocardial Infarction Model Using PET. Journal of Nuclear Medicine, 2008, 49, 667-673.	5.0	102
89	Positron Emission Tomography Imaging of CD105 Expression with a 64Cu-Labeled Monoclonal Antibody: NOTA Is Superior to DOTA. PLoS ONE, 2011, 6, e28005.	2.5	101
90	89Zr-labeled nivolumab for imaging of T-cell infiltration in a humanized murine model of lung cancer. European Journal of Nuclear Medicine and Molecular Imaging, 2018, 45, 110-120.	6.4	100

#	Article	IF	CITATIONS
91	Image-guided and tumor-targeted drug delivery with radiolabeled unimolecular micelles. Biomaterials, 2013, 34, 8323-8332.	11.4	98
92	Positron Emission Tomography Image-Guided Drug Delivery: Current Status and Future Perspectives. Molecular Pharmaceutics, 2014, 11, 3777-3797.	4.6	93
93	Molecular Imaging with SERSâ€Active Nanoparticles. Small, 2011, 7, 3261-3269.	10.0	92
94	Theranostic Unimolecular Micelles Based on Brush-Shaped Amphiphilic Block Copolymers for Tumor-Targeted Drug Delivery and Positron Emission Tomography Imaging. ACS Applied Materials & Interfaces, 2014, 6, 21769-21779.	8.0	92
95	PET imaging of colorectal cancer in xenograft-bearing mice by use of an 18F-labeled T84.66 anti-carcinoembryonic antigen diabody. Journal of Nuclear Medicine, 2007, 48, 304-10.	5.0	92
96	Collagen Mimetic Dendrimers. Journal of the American Chemical Society, 2002, 124, 15162-15163.	13.7	91
97	Radiotheranostics in Cancer Diagnosis and Management. Radiology, 2018, 286, 388-400.	7.3	91
98	In Vivo Tumor Vasculature Targeted PET/NIRF Imaging with TRC105(Fab)-Conjugated, Dual-Labeled Mesoporous Silica Nanoparticles. Molecular Pharmaceutics, 2014, 11, 4007-4014.	4.6	90
99	Ultra-small iron-gallic acid coordination polymer nanoparticles for chelator-free labeling of ⁶⁴ Cu and multimodal imaging-guided photothermal therapy. Nanoscale, 2017, 9, 12609-12617.	5.6	90
100	Self-Activated Electrical Stimulation for Effective Hair Regeneration <i>via</i> a Wearable Omnidirectional Pulse Generator. ACS Nano, 2019, 13, 12345-12356.	14.6	90
101	Multimodality imaging of vascular endothelial growth factor and vascular endothelial growth factor receptor expression. Frontiers in Bioscience - Landmark, 2007, 12, 4267.	3.0	89
102	Dual-Modality Positron Emission Tomography/Optical Image-Guided Photodynamic Cancer Therapy with Chlorin e6-Containing Nanomicelles. ACS Nano, 2016, 10, 7721-7730.	14.6	88
103	Noninvasive PET Imaging of T cells. Trends in Cancer, 2018, 4, 359-373.	7.4	88
104	Molecular Imaging with Nucleic Acid Aptamers. Current Medicinal Chemistry, 2011, 18, 4195-4205.	2.4	87
105	⁴⁴ Sc: An Attractive Isotope for Peptide-Based PET Imaging. Molecular Pharmaceutics, 2014, 11, 2954-2961.	4.6	87
106	Non-Invasive Cell Tracking in Cancer and Cancer Therapy. Current Topics in Medicinal Chemistry, 2010, 10, 1237-1248.	2.1	86
107	Reassembly of ⁸⁹ Zr‣abeled Cancer Cell Membranes into Multicompartment Membraneâ€Derived Liposomes for PETâ€Trackable Tumorâ€Targeted Theranostics. Advanced Materials, 2018, 30, e1704934.	21.0	86
108	Biomedical applications of functionalized hollow mesoporous silica nanoparticles: focusing on molecular imaging. Nanomedicine, 2013, 8, 2027-2039.	3.3	85

#	Article	IF	CITATIONS
109	Efficient Uptake of ¹⁷⁷ Luâ€Porphyrinâ€PEG Nanocomplexes by Tumor Mitochondria for Multimodalâ€Imagingâ€Guided Combination Therapy. Angewandte Chemie - International Edition, 2018, 57, 218-222.	13.8	85
110	Multimodality molecular imaging of glioblastoma growth inhibition with vasculature-targeting fusion toxin VEGF121/rGel. Journal of Nuclear Medicine, 2007, 48, 445-54.	5.0	85
111	Red Fluorescent Zinc Oxide Nanoparticle: A Novel Platform for Cancer Targeting. ACS Applied Materials & Interfaces, 2015, 7, 3373-3381.	8.0	84
112	ImmunoPET Imaging of CTLA-4 Expression in Mouse Models of Non-small Cell Lung Cancer. Molecular Pharmaceutics, 2017, 14, 1782-1789.	4.6	84
113	Plumbagin, a medicinal plant (<i>lumbago zeylanica</i>)â€derived 1,4â€naphthoquinone, inhibits growth and metastasis of human prostate cancer PCâ€3Mâ€luciferase cells in an orthotopic xenograft mouse model. Molecular Oncology, 2013, 7, 428-439.	4.6	82
114	Semiconductor Quantum Dots for <i>In Vivo</i> Imaging. Journal of Nanoscience and Nanotechnology, 2007, 7, 2567-2581.	0.9	80
115	⁵² Mn Production for PET/MRI Tracking Of Human Stem Cells Expressing Divalent Metal Transporter 1 (DMT1). Theranostics, 2015, 5, 227-239.	10.0	80
116	Hollow mesoporous silica nanoparticles for tumor vasculature targeting and PET image-guided drug delivery. Nanomedicine, 2015, 10, 1233-1246.	3.3	80
117	Integrin αvβ3-Targeted Radioimmunotherapy of Glioblastoma Multiforme. Clinical Cancer Research, 2008, 14, 7330-7339.	7.0	79
118	Quantitative radioimmunoPET imaging of EphA2 in tumor-bearing mice. European Journal of Nuclear Medicine and Molecular Imaging, 2007, 34, 2024-2036.	6.4	77
119	Positron emission tomography imaging of CD105 expression during tumor angiogenesis. European Journal of Nuclear Medicine and Molecular Imaging, 2011, 38, 1335-1343.	6.4	77
120	Molecular Imaging of Immunotherapy Targets in Cancer. Journal of Nuclear Medicine, 2016, 57, 1487-1492.	5.0	77
121	Radiolabeling Silica-Based Nanoparticles via Coordination Chemistry: Basic Principles, Strategies, and Applications. Accounts of Chemical Research, 2018, 51, 778-788.	15.6	77
122	Chiralityâ€Driven Transportation and Oxidation Prevention by Chiral Selenium Nanoparticles. Angewandte Chemie - International Edition, 2020, 59, 4406-4414.	13.8	77
123	Positron emission tomography imaging of CD105 expression with 89Zr-Df-TRC105. European Journal of Nuclear Medicine and Molecular Imaging, 2012, 39, 138-148.	6.4	75
124	Matching the Decay Half-Life with the Biological Half-Life: ImmunoPET Imaging with ⁴⁴ Sc-Labeled Cetuximab Fab Fragment. Bioconjugate Chemistry, 2014, 25, 2197-2204.	3.6	74
125	Novel Preparation Methods of ⁵² Mn for ImmunoPET Imaging. Bioconjugate Chemistry, 2015, 26, 2118-2124.	3.6	74
126	Renal-Clearable Ultrasmall Coordination Polymer Nanodots for Chelator-Free ⁶⁴ Cu-Labeling and Imaging-Guided Enhanced Radiotherapy of Cancer. ACS Nano, 2017, 11, 9103-9111.	14.6	73

#	Article	IF	CITATIONS
127	VEGFR targeting leads to significantly enhanced tumor uptake of nanographene oxide inÂvivo. Biomaterials, 2015, 39, 39-46.	11.4	72
128	Quantitative PET Imaging of VEGF Receptor Expression. Molecular Imaging and Biology, 2009, 11, 15-22.	2.6	71
129	A self-powered implantable and bioresorbable electrostimulation device for biofeedback bone fracture healing. Proceedings of the National Academy of Sciences of the United States of America, 2021, 118, .	7.1	71
130	Engineering Intrinsically Zirconiumâ€89 Radiolabeled Selfâ€Destructing Mesoporous Silica Nanostructures for In Vivo Biodistribution and Tumor Targeting Studies. Advanced Science, 2016, 3, 1600122.	11.2	70
131	Monitoring of the Biological Response to Murine Hindlimb Ischemia With ⁶⁴ Cu-Labeled Vascular Endothelial Growth Factor-121 Positron Emission Tomography. Circulation, 2008, 117, 915-922.	1.6	69
132	Tumor Vasculature Targeting: A Generally Applicable Approach for Functionalized Nanomaterials. Small, 2014, 10, 1887-1893.	10.0	69
133	A Novel Fusion of ALT-803 (Interleukin (IL)-15 Superagonist) with an Antibody Demonstrates Antigen-specific Antitumor Responses. Journal of Biological Chemistry, 2016, 291, 23869-23881.	3.4	68
134	Surfactant‣tripped Frozen Pheophytin Micelles for Multimodal Gut Imaging. Advanced Materials, 2016, 28, 8524-8530.	21.0	67
135	Study of long-term biocompatibility and bio-safety of implantable nanogenerators. Nano Energy, 2018, 51, 728-735.	16.0	67
136	Photoacoustic Imaging. Cold Spring Harbor Protocols, 2011, 2011, pdb.top065508.	0.3	66
137	Dynamic Positron Emission Tomography Imaging of Renal Clearable Gold Nanoparticles. Small, 2016, 12, 2775-2782.	10.0	66
138	Chelatorâ€Free Radiolabeling of Nanographene: Breaking the Stereotype of Chelation. Angewandte Chemie - International Edition, 2017, 56, 2889-2892.	13.8	65
139	PET imaging of acute and chronic inflammation in living mice. European Journal of Nuclear Medicine and Molecular Imaging, 2007, 34, 1832-1842.	6.4	63
140	Multimodality Imaging of Breast Cancer Experimental Lung Metastasis with Bioluminescence and a Monoclonal Antibody Dual-Labeled with ⁸⁹ Zr and IRDye 800CW. Molecular Pharmaceutics, 2012, 9, 2339-2349.	4.6	63
141	Molecular Imaging of Pancreatic Cancer with Antibodies. Molecular Pharmaceutics, 2016, 13, 8-24.	4.6	62
142	Intrabilayer ⁶⁴ Cu Labeling of Photoactivatable, Doxorubicin-Loaded Stealth Liposomes. ACS Nano, 2017, 11, 12482-12491.	14.6	62
143	Multimodality Imaging Agents with PET as the Fundamental Pillar. Angewandte Chemie - International Edition, 2019, 58, 2570-2579.	13.8	62
144	Selfâ€Amplified Photodynamic Therapy through the ¹ O ₂ â€Mediated Internalization of Photosensitizers from a Ppaâ€Bearing Block Copolymer. Angewandte Chemie - International Edition, 2020, 59, 3711-3717.	13.8	62

#	Article	IF	CITATIONS
145	Re-assessing the enhanced permeability and retention effect in peripheral arterial disease using radiolabeled long circulating nanoparticles. Biomaterials, 2016, 100, 101-109.	11.4	61
146	Positron Emission Tomography and Near-Infrared Fluorescence Imaging of Vascular Endothelial Growth Factor with Dual-Labeled Bevacizumab. American Journal of Nuclear Medicine and Molecular Imaging, 2012, 2, 1-13.	1.0	61
147	Positron emission tomography imaging of prostate cancer. Amino Acids, 2010, 39, 11-27.	2.7	60
148	A porphyrin-PEG polymer with rapid renal clearance. Biomaterials, 2016, 76, 25-32.	11.4	60
149	Aptamers as Therapeutics in Cardiovascular Diseases. Current Medicinal Chemistry, 2011, 18, 4169-4174.	2.4	59
150	Quantum Dot-Based Nanoprobes for In Vivo Targeted Imaging. Current Molecular Medicine, 2013, 13, 1549-1567.	1.3	59
151	Long circulating reduced graphene oxide–iron oxide nanoparticles for efficient tumor targeting and multimodality imaging. Nanoscale, 2016, 8, 12683-12692.	5.6	58
152	Applications of Aptamers in Targeted Imaging: State of the Art. Current Topics in Medicinal Chemistry, 2015, 15, 1138-1152.	2.1	58
153	Noninvasive <i>De novo</i> Imaging of Human Embryonic Stem Cell–Derived Teratoma Formation. Cancer Research, 2009, 69, 2709-2713.	0.9	57
154	CD146-targeted immunoPET and NIRF Imaging of Hepatocellular Carcinoma with a Dual-Labeled Monoclonal Antibody. Theranostics, 2016, 6, 1918-1933.	10.0	57
155	DNA nanomaterials for preclinical imaging and drug delivery. Journal of Controlled Release, 2016, 239, 27-38.	9.9	57
156	Nanomedicines for Renal Management: From Imaging to Treatment. Accounts of Chemical Research, 2020, 53, 1869-1880.	15.6	57
157	A highly hemocompatible erythrocyte membrane-coated ultrasmall selenium nanosystem for simultaneous cancer radiosensitization and precise antiangiogenesis. Journal of Materials Chemistry B, 2018, 6, 4756-4764.	5.8	56
158	Multimodality tumor imaging targeting integrin α _v β ₃ . BioTechniques, 2005, 39, S14-S25.	1.8	55
159	Imaging of Abdominal Aortic Aneurysm: The Present and the Future. Current Vascular Pharmacology, 2010, 8, 808-819.	1.7	55
160	Smart H ₂ Sâ€īriggered/Therapeutic System (SHTS)â€Based Nanomedicine. Advanced Science, 2019, 6, 1901724.	11.2	55
161	Noninvasive brain cancer imaging with a bispecific antibody fragment, generated via click chemistry. Proceedings of the National Academy of Sciences of the United States of America, 2015, 112, 12806-12811.	7.1	54
162	Targeting CD146 with a ⁶⁴ Cu-labeled antibody enables in vivo immunoPET imaging of high-grade gliomas. Proceedings of the National Academy of Sciences of the United States of America, 2015, 112, E6525-34.	7.1	54

#	Article	IF	CITATIONS
163	Implanted Battery-Free Direct-Current Micro-Power Supply from in Vivo Breath Energy Harvesting. ACS Applied Materials & Interfaces, 2018, 10, 42030-42038.	8.0	54
164	Vascular Endothelial Growth Factor and Vascular Endothelial Growth Factor Receptor Inhibitors as Anti-Angiogenic Agents in Cancer Therapy. Recent Patents on Anti-Cancer Drug Discovery, 2007, 2, 59-71.	1.6	53
165	Integrin-targeted imaging and therapy with RGD4C-TNF fusion protein. Molecular Cancer Therapeutics, 2008, 7, 1044-1053.	4.1	53
166	$\label{eq:maging} Multimodality Imaging of Integrin \ \hat{l} \pm < sub > v < / sub > \hat{l}^2 < sub > 3 < / sub > Expression. The random stics, 2011, 1, 135-148.$	10.0	53
167	Quantum dot–NanoLuc bioluminescence resonance energy transfer enables tumor imaging and lymph node mapping in vivo. Chemical Communications, 2016, 52, 6997-7000.	4.1	53
168	Intrathecal Administration of Nanoclusters for Protecting Neurons against Oxidative Stress in Cerebral Ischemia/Reperfusion Injury. ACS Nano, 2019, 13, 13382-13389.	14.6	53
169	Integrin αvβ3 Antagonists for Anti-Angiogenic Cancer Treatment. Recent Patents on Anti-Cancer Drug Discovery, 2007, 2, 143-158.	1.6	52
170	Chelator-Free Labeling of Layered Double Hydroxide Nanoparticles for in Vivo PET Imaging. Scientific Reports, 2015, 5, 16930.	3.3	52
171	Multimodality imaging of nitric oxide and nitric oxide synthases. Free Radical Biology and Medicine, 2009, 47, 684-698.	2.9	51
172	Aptamer-Conjugated Framework Nucleic Acids for the Repair of Cerebral Ischemia-Reperfusion Injury. Nano Letters, 2019, 19, 7334-7341.	9.1	51
173	Molecular Imaging of Proteases in Cancer. Cancer Growth and Metastasis, 2009, 2, CGM.S2814.	3.5	49
174	Immuno-PET of Tissue Factor in Pancreatic Cancer. Journal of Nuclear Medicine, 2012, 53, 1748-1754.	5.0	49
175	Accelerated Blood Clearance Phenomenon Reduces the Passive Targeting of PEGylated Nanoparticles in Peripheral Arterial Disease. ACS Applied Materials & Interfaces, 2016, 8, 17955-17963.	8.0	48
176	Openâ€ 5 hell Nanosensitizers for Glutathione Responsive Cancer Sonodynamic Therapy. Advanced Materials, 2022, 34, e2110283.	21.0	48
177	Metal-assisted Assembly and Stabilization of Collagen-like Triple Helices. Journal of the American Chemical Society, 2004, 126, 15030-15031.	13.7	47
178	Positron Emission Tomography Imaging of Poststroke Angiogenesis. Stroke, 2009, 40, 270-277.	2.0	47
179	PET imaging of CD105/endoglin expression with a 61/64Cu-labeled Fab antibody fragment. European Journal of Nuclear Medicine and Molecular Imaging, 2013, 40, 759-767.	6.4	47
180	New radiotracers for imaging of vascular targets in angiogenesis-related diseases. Advanced Drug Delivery Reviews, 2014, 76, 2-20.	13.7	47

#	Article	IF	CITATIONS
181	Intrinsic radiolabeling of Titanium-45 using mesoporous silica nanoparticles. Acta Pharmacologica Sinica, 2017, 38, 907-913.	6.1	47
182	Radiolabeled, Antibody-Conjugated Manganese Oxide Nanoparticles for Tumor Vasculature Targeted Positron Emission Tomography and Magnetic Resonance Imaging. ACS Applied Materials & Interfaces, 2017, 9, 38304-38312.	8.0	47
183	Photo-Enhanced Singlet Oxygen Generation of Prussian Blue-Based Nanocatalyst for Augmented Photodynamic Therapy. IScience, 2018, 9, 14-26.	4.1	46
184	Multifunctional Artificial Artery from Direct 3D Printing with Builtâ€In Ferroelectricity and Tissueâ€Matching Modulus for Realâ€Time Sensing and Occlusion Monitoring. Advanced Functional Materials, 2020, 30, 2002868.	14.9	46
185	Engineering of radiolabeled iron oxide nanoparticles for dualâ€modality imaging. Wiley Interdisciplinary Reviews: Nanomedicine and Nanobiotechnology, 2016, 8, 619-630.	6.1	43
186	PET radiometals for antibody labeling. Journal of Labelled Compounds and Radiopharmaceuticals, 2018, 61, 636-651.	1.0	43
187	Radionuclideâ€Activated Nanomaterials and Their Biomedical Applications. Angewandte Chemie - International Edition, 2019, 58, 13232-13252.	13.8	43
188	Sulfoxideâ€Containing Polymerâ€Coated Nanoparticles Demonstrate Minimal Protein Fouling and Improved Blood Circulation. Advanced Science, 2020, 7, 2000406.	11.2	43
189	Clinical summary of fibroblast activation protein inhibitor-based radiopharmaceuticals: cancer and beyond. European Journal of Nuclear Medicine and Molecular Imaging, 2022, 49, 2844-2868.	6.4	43
190	Radiolabeled polyoxometalate clusters: Kidney dysfunction evaluation and tumor diagnosis by positron emission tomography imaging. Biomaterials, 2018, 171, 144-152.	11.4	42
191	Molecular imaging of β-cells: diabetes and beyond. Advanced Drug Delivery Reviews, 2019, 139, 16-31.	13.7	42
192	CD146â€Targeted Multimodal Imageâ€Guided Photoimmunotherapy of Melanoma. Advanced Science, 2019, 6, 1801237.	11.2	42
193	Image-Guided Drug Delivery with Single-Photon Emission Computed Tomography: A Review of Literature. Current Drug Targets, 2015, 16, 592-609.	2.1	42
194	Multimodality molecular imaging of CD105 (Endoglin) expression. International Journal of Clinical and Experimental Medicine, 2011, 4, 32-42.	1.3	42
195	Non-Invasive PET Imaging of EGFR Degradation Induced by a Heat Shock Protein 90 Inhibitor. Molecular Imaging and Biology, 2008, 10, 99-106.	2.6	41
196	Site-Specific Immuno-PET Tracer to Image PD-L1. Molecular Pharmaceutics, 2019, 16, 2028-2036.	4.6	41
197	Intrinsic and Stable Conjugation of Thiolated Mesoporous Silica Nanoparticles with Radioarsenic. ACS Applied Materials & Interfaces, 2017, 9, 6772-6781.	8.0	40
198	Positron Emission Tomography and Optical Imaging of Tumor CD105 Expression with a Dual-Labeled Monoclonal Antibody. Molecular Pharmaceutics, 2012, 9, 645-653.	4.6	39

#	Article	IF	CITATIONS
199	High Yield Production and Radiochemical Isolation of Isotopically Pure Arsenic-72 and Novel Radioarsenic Labeling Strategies for the Development of Theranostic Radiopharmaceuticals. Bioconjugate Chemistry, 2016, 27, 179-188.	3.6	39
200	Sizeâ€Optimized Ultrasmall Porous Silica Nanoparticles Depict Vasculatureâ€Based Differential Targeting in Triple Negative Breast Cancer. Small, 2019, 15, e1903747.	10.0	39
201	Surfactant-stripped naphthalocyanines for multimodal tumor theranostics with upconversion guidance cream. Nanoscale, 2017, 9, 3391-3398.	5.6	38
202	ImmunoPET and near-infrared fluorescence imaging of CD105 expression using a monoclonal antibody dual-labeled with (89)Zr and IRDye 800CW. American Journal of Translational Research (discontinued), 2012, 4, 333-46.	0.0	38
203	Chapter 7 Molecular Imaging of Tumor Vasculature. Methods in Enzymology, 2008, 445, 141-176.	1.0	37
204	In vivo near-infrared fluorescence imaging of CD105 expression during tumor angiogenesis. European Journal of Nuclear Medicine and Molecular Imaging, 2011, 38, 2066-2076.	6.4	37
205	Positron Emission Tomography Imaging of Tumor Angiogenesis with a ⁶⁶ Ga-Labeled Monoclonal Antibody. Molecular Pharmaceutics, 2012, 9, 1441-1448.	4.6	37
206	PET/SPECT imaging of hindlimb ischemia: focusing on angiogenesis and blood flow. Angiogenesis, 2013, 16, 279-287.	7.2	37
207	Radiolabeled inorganic nanoparticles for positron emission tomography imaging of cancer: an overview. Quarterly Journal of Nuclear Medicine and Molecular Imaging, 2017, 61, 181-204.	0.7	37
208	Dual-Targeted Molecular Imaging of Cancer. Journal of Nuclear Medicine, 2018, 59, 390-395.	5.0	37
209	Radionuclide-Based Cancer Imaging Targeting the Carcinoembryonic Antigen. Biomarker Insights, 2008, 3, BMI.S1124.	2.5	36
210	Positron Emission Tomography Imaging of Tumor Angiogenesis with a ^{61/64} Cu-Labeled F(ab′) ₂ Antibody Fragment. Molecular Pharmaceutics, 2013, 10, 709-716.	4.6	36
211	Positron Emission Tomography Imaging of Atherosclerosis. Theranostics, 2013, 3, 894-902.	10.0	36
212	ImmunoPET of tissue factor expression in triple-negative breast cancer with a radiolabeled antibody Fab fragment. European Journal of Nuclear Medicine and Molecular Imaging, 2015, 42, 1295-1303.	6.4	36
213	ImmunoPET and Near-Infrared Fluorescence Imaging of Pancreatic Cancer with a Dual-Labeled Bispecific Antibody Fragment. Molecular Pharmaceutics, 2017, 14, 1646-1655.	4.6	36
214	Targeting and microenvironment-improving of phenylboronic acid-decorated soy protein nanoparticles with different sizes to tumor. Theranostics, 2019, 9, 7417-7430.	10.0	36
215	In Vivo Imaging of RNA Interference. Journal of Nuclear Medicine, 2010, 51, 169-172.	5.0	35
216	PET Imaging of Abdominal Aortic Aneurysm with ⁶⁴ Cu-Labeled Anti-CD105 Antibody Fab Fragment. Journal of Nuclear Medicine, 2015, 56, 927-932.	5.0	35

#	Article	IF	CITATIONS
217	PET Imaging of Receptor Tyrosine Kinases in Cancer. Molecular Cancer Therapeutics, 2018, 17, 1625-1636.	4.1	35
218	A "Missileâ€Ðetonation―Strategy to Precisely Supply and Efficiently Amplify Cerenkov Radiation Energy for Cancer Theranostics. Advanced Materials, 2019, 31, e1904894.	21.0	35
219	Internally Responsive Nanomaterials for Activatable Multimodal Imaging of Cancer. Advanced Healthcare Materials, 2021, 10, e2000690.	7.6	35
220	Multimodality Imaging of IL-18–Binding Protein-Fc Therapy of Experimental Lung Metastasis. Clinical Cancer Research, 2008, 14, 6137-6145.	7.0	34
221	Evolution of zinc oxide nanostructures through kinetics control. Journal of Materials Chemistry, 2011, 21, 9000.	6.7	34
222	α- Versus β-Emitting Radionuclides for Pretargeted Radioimmunotherapy of Carcinoembryonic Antigen–Expressing Human Colon Cancer Xenografts. Journal of Nuclear Medicine, 2017, 58, 926-933.	5.0	34
223	Chelator-Free Labeling of Metal Oxide Nanostructures with Zirconium-89 for Positron Emission Tomography Imaging. ACS Nano, 2017, 11, 12193-12201.	14.6	34
224	Noninvasive Imaging and Quantification of Radiotherapy-Induced PD-L1 Upregulation with ⁸⁹ Zr–Df–Atezolizumab. Bioconjugate Chemistry, 2019, 30, 1434-1441.	3.6	34
225	Efficient renal clearance of DNA tetrahedron nanoparticles enables quantitative evaluation of kidney function. Nano Research, 2019, 12, 637-642.	10.4	34
226	HPMA-based star polymer biomaterials with tuneable structure and biodegradability tailored for advanced drug delivery to solid tumours. Biomaterials, 2020, 235, 119728.	11.4	33
227	Combination of integrin siRNA and irradiation for breast cancer therapy. Biochemical and Biophysical Research Communications, 2006, 351, 726-732.	2.1	32
228	Intrinsically Zirconium-89 Labeled Gd ₂ O ₂ S:Eu Nanoprobes for In Vivo Positron Emission Tomography and Gamma-Ray-Induced Radioluminescence Imaging. Small, 2016, 12, 2872-2876.	10.0	32
229	Radiomanganese PET Detects Changes in Functional β-Cell Mass in Mouse Models of Diabetes. Diabetes, 2017, 66, 2163-2174.	0.6	32
230	Prevention of Hepatic Ischemia-Reperfusion Injury by Carbohydrate-Derived Nanoantioxidants. Nano Letters, 2020, 20, 6510-6519.	9.1	32
231	Design and Applications of Bispecific Heterodimers: Molecular Imaging and beyond. Molecular Pharmaceutics, 2014, 11, 1750-1761.	4.6	31
232	Facile Preparation of Multifunctional WS ₂ /WO <i>_x</i> Nanodots for Chelator-Free ⁸⁹ Zr-Labeling and In Vivo PET Imaging. Small, 2016, 12, 5750-5758.	10.0	31
233	Radiolabeled pertuzumab for imaging of human epidermal growth factor receptor 2 expression in ovarian cancer. European Journal of Nuclear Medicine and Molecular Imaging, 2017, 44, 1296-1305.	6.4	31
234	Evaluation of the biological activities of the IL-15 superagonist complex, ALT-803, following intravenous versus subcutaneous administration in murine models. Cytokine, 2018, 107, 105-112.	3.2	31

#	Article	IF	CITATIONS
235	In Vivo Tumor-Targeted Dual-Modality PET/Optical Imaging with a Yolk/Shell-Structured Silica Nanosystem. Nano-Micro Letters, 2018, 10, 65.	27.0	31
236	Astrocyte-Neuron Signaling in Synaptogenesis. Frontiers in Cell and Developmental Biology, 2021, 9, 680301.	3.7	31
237	Molecular imaging of human epidermal growth factor receptor 2 (HER-2) expression. Frontiers in Bioscience - Landmark, 2008, 13, 790.	3.0	31
238	In Vivo Bioluminescence Tumor Imaging of RGD Peptide-modified Adenoviral Vector Encoding Firefly Luciferase Reporter Gene. Molecular Imaging and Biology, 2007, 9, 126-134.	2.6	30
239	Dual Targeting of Tissue Factor and CD105 for Preclinical PET Imaging of Pancreatic Cancer. Clinical Cancer Research, 2016, 22, 3821-3830.	7.0	30
240	PET Imaging of VEGFR-2 Expression in Lung Cancer with ⁶⁴ Cu-Labeled Ramucirumab. Journal of Nuclear Medicine, 2016, 57, 285-290.	5.0	30
241	ImmunoPET imaging of CD38 in murine lymphoma models using 89Zr-labeled daratumumab. European Journal of Nuclear Medicine and Molecular Imaging, 2018, 45, 1372-1381.	6.4	30
242	Ultrasmall Porous Silica Nanoparticles with Enhanced Pharmacokinetics for Cancer Theranostics. Nano Letters, 2021, 21, 4692-4699.	9.1	30
243	Imaging of Induced Pluripotent Stem Cells: From Cellular Reprogramming to Transplantation. American Journal of Nuclear Medicine and Molecular Imaging, 2011, 1, 18-28.	1.0	30
244	A tumor-targeted polymer theranostics platform for positron emission tomography and fluorescence imaging. Nanoscale, 2017, 9, 10906-10918.	5.6	29
245	PET and SPECT imaging of melanoma: the state of the art. European Journal of Nuclear Medicine and Molecular Imaging, 2018, 45, 132-150.	6.4	29
246	Intrinsically Zirconium-89-Labeled Manganese Oxide Nanoparticles for <i>In Vivo</i> Dual-Modality Positron Emission Tomography and Magnetic Resonance Imaging. Journal of Biomedical Nanotechnology, 2018, 14, 900-909.	1.1	29
247	Production and in vivo PET/CT imaging of the theranostic pair 132/135La. Scientific Reports, 2019, 9, 10658.	3.3	29
248	Imaging tumor angiogenesis in breast cancer experimental lung metastasis with positron emission tomography, near-infrared fluorescence, and bioluminescence. Angiogenesis, 2013, 16, 663-674.	7.2	28
249	Pharmacokinetic Issues of Imaging with Nanoparticles: Focusing on Carbon Nanotubes and Quantum Dots. Molecular Imaging and Biology, 2013, 15, 507-520.	2.6	28
250	General synthesis of silica-based yolk/shell hybrid nanomaterials and in vivo tumor vasculature targeting. Nano Research, 2018, 11, 4890-4904.	10.4	28
251	In a "nutshell": intrinsically radio-labeled quantum dots. American Journal of Nuclear Medicine and Molecular Imaging, 2012, 2, 136-40.	1.0	28
252	Radiolabeled Î ³ -AApeptides: a new class of tracers for positron emission tomography. Chemical Communications, 2012, 48, 7850.	4.1	26

#	Article	IF	CITATIONS
253	Positron Emission Tomography Imaging of Angiogenesis in a Murine Hindlimb Ischemia Model with ⁶⁴ Cu-Labeled TRC105. Molecular Pharmaceutics, 2013, 10, 2749-2756.	4.6	25
254	ImmunoPET Imaging of CD146 Expression in Malignant Brain Tumors. Molecular Pharmaceutics, 2016, 13, 2563-2570.	4.6	25
255	CD38 as a PET Imaging Target in Lung Cancer. Molecular Pharmaceutics, 2017, 14, 2400-2406.	4.6	25
256	Monoclonal Antibody against CXCL1 (HL2401) as a Novel Agent in Suppressing IL6 Expression and Tumoral Growth. Theranostics, 2019, 9, 853-867.	10.0	25
257	Exploiting Nanomaterialâ€Mediated Autophagy for Cancer Therapy. Small Methods, 2019, 3, 1800365.	8.6	25
258	Targeted α-therapy of prostate cancer using radiolabeled PSMA inhibitors: a game changer in nuclear medicine. American Journal of Nuclear Medicine and Molecular Imaging, 2018, 8, 247-267.	1.0	25
259	Moving Beyond the Pillars of Cancer Treatment: Perspectives From Nanotechnology. Frontiers in Chemistry, 2020, 8, 598100.	3.6	24
260	PET of Follicle-Stimulating Hormone Receptor: Broad Applicability to Cancer Imaging. Molecular Pharmaceutics, 2015, 12, 403-410.	4.6	23
261	ImmunoPET for assessing the differential uptake of a CD146-specific monoclonal antibody in lung cancer. European Journal of Nuclear Medicine and Molecular Imaging, 2016, 43, 2169-2179.	6.4	23
262	Antibodyâ€Based Tracers for PET/SPECT Imaging of Chronic Inflammatory Diseases. ChemBioChem, 2019, 20, 422-436.	2.6	23
263	[^{nat/44} Sc(pypa)] ^{â^} : Thermodynamic Stability, Radiolabeling, and Biodistribution of a Prostate-Specific-Membrane-Antigen-Targeting Conjugate. Inorganic Chemistry, 2020, 59, 1985-1995.	4.0	23
264	Peptoid and Positron Emission Tomography: an Appealing Combination. American Journal of Nuclear Medicine and Molecular Imaging, 2011, 1, 76-79.	1.0	23
265	The temporal correlation of dynamic contrast-enhanced magnetic resonance imaging with tumor angiogenesis in a murine glioblastoma model. Neurological Research, 2008, 30, 952-959.	1.3	22
266	Anatomical and molecular imaging of skin cancer. Clinical, Cosmetic and Investigational Dermatology, 2008, 1, 1.	1.8	22
267	Uptake and retention of manganese contrast agents for PET and MRI in the rodent brain. Contrast Media and Molecular Imaging, 2016, 11, 371-380.	0.8	22
268	Preparation and in vivo characterization of 51MnCl2 as PET tracer of Ca2+ channel-mediated transport. Scientific Reports, 2017, 7, 3033.	3.3	22
269	Preventing Radiobleaching of Cyanine Fluorophores Enhances Stability of Nuclear/NIRF Multimodality Imaging Agents. Theranostics, 2017, 7, 1-8.	10.0	22
270	Chiralityâ€Driven Transportation and Oxidation Prevention by Chiral Selenium Nanoparticles. Angewandte Chemie, 2020, 132, 4436-4444.	2.0	22

#	Article	IF	CITATIONS
271	Tissue Factorâ€Targeted ImmunoPET Imaging and Radioimmunotherapy of Anaplastic Thyroid Cancer. Advanced Science, 2020, 7, 1903595.	11.2	22
272	Non-Invasive Imaging of Human Embryonic Stem Cells. Current Pharmaceutical Biotechnology, 2010, 11, 685-692.	1.6	21
273	PET of c-Met in Cancer with ⁶⁴ Cu-Labeled Hepatocyte Growth Factor. Journal of Nuclear Medicine, 2015, 56, 758-763.	5.0	21
274	Lymphoma: current status of clinical and preclinical imaging with radiolabeled antibodies. European Journal of Nuclear Medicine and Molecular Imaging, 2017, 44, 517-532.	6.4	21
275	Noninvasive Evaluation of CD20 Expression Using ⁶⁴ Cu-Labeled F(ab′) ₂ Fragments of Obinutuzumab in Lymphoma. Journal of Nuclear Medicine, 2021, 62, 372-378.	5.0	21
276	Spherical nucleic acids: Organized nucleotide aggregates as versatile nanomedicine. Aggregate, 2022, 3, e120.	9.9	21
277	"Albumin Hitchhiking―with an Evans Blue Analog for Cancer Theranostics. Theranostics, 2018, 8, 812-814.	10.0	20
278	CD38â€Targeted Theranostics of Lymphoma with ⁸⁹ Zr/ ¹⁷⁷ Lu‣abeled Daratumumab. Advanced Science, 2021, 8, 2001879.	11.2	20
279	HaloTag: a novel reporter gene for positron emission tomography. American Journal of Translational Research (discontinued), 2011, 3, 392-403.	0.0	20
280	Intracellular signaling pathway in dendritic cells and antigen transport pathway in vivo mediated by an OVA@DDAB/PLGA nano-vaccine. Journal of Nanobiotechnology, 2021, 19, 394.	9.1	20
281	Targeted Cancer Therapy with Tumor Necrosis Factor-Alpha. Biochemistry Insights, 2008, 1, BCI.S901.	3.3	19
282	ImmunoPET imaging of tissue factor expression in pancreatic cancer with 89Zr-Df-ALT-836. Journal of Controlled Release, 2017, 264, 160-168.	9.9	19
283	Noninvasive Trafficking of Brentuximab Vedotin and PET Imaging of CD30 in Lung Cancer Murine Models. Molecular Pharmaceutics, 2018, 15, 1627-1634.	4.6	19
284	86/90Y-Based Theranostics Targeting Angiogenesis in a Murine Breast Cancer Model. Molecular Pharmaceutics, 2018, 15, 2606-2613.	4.6	19
285	86/90Y-Labeled Monoclonal Antibody Targeting Tissue Factor for Pancreatic Cancer Theranostics. Molecular Pharmaceutics, 2020, 17, 1697-1705.	4.6	19
286	Responsive hyaluronic acid-gold cluster hybrid nanogel theranostic systems. Biomaterials Science, 2021, 9, 1363-1373.	5.4	19
287	Long-term in vivo operation of implanted cardiac nanogenerators in swine. Nano Energy, 2021, 90, 106507.	16.0	19
288	Antibody and fragment-based PET imaging of CTLA-4+ T-cells in humanized mouse models. American Journal of Cancer Research, 2019, 9, 53-63.	1.4	19

#	Article	IF	CITATIONS
289	ImmunoPET of trophoblast cell-surface antigen 2 (Trop-2) expression in pancreatic cancer. European Journal of Nuclear Medicine and Molecular Imaging, 2022, 49, 861-870.	6.4	18
290	Multimodality Imaging of CXCR4 in Cancer: Current Status towards Clinical Translation. Current Molecular Medicine, 2013, 13, 1538-1548.	1.3	18
291	Radionuclide-Based Imaging of Breast Cancer: State of the Art. Cancers, 2021, 13, 5459.	3.7	18
292	Evaluation of two novel 64Cu-labeled RGD peptide radiotracers for enhanced PET imaging of tumor integrin αvβ3. European Journal of Nuclear Medicine and Molecular Imaging, 2015, 42, 1859-1868.	6.4	17
293	Targeting angiogenesis for radioimmunotherapy with a 177Lu-labeled antibody. European Journal of Nuclear Medicine and Molecular Imaging, 2018, 45, 123-131.	6.4	17
294	In vitro study of enhanced photodynamic cancer cell killing effect by nanometer-thick gold nanosheets. Nano Research, 2020, 13, 3217-3223.	10.4	17
295	Intraoperative Targeted Optical Imaging: A Guide towards Tumor-Free Margins in Cancer Surgery. Current Pharmaceutical Biotechnology, 2014, 14, 733-742.	1.6	17
296	Nanostructured polyvinylpyrrolidone-curcumin conjugates allowed for kidney-targeted treatment of cisplatin induced acute kidney injury. Bioactive Materials, 2023, 19, 282-291.	15.6	17
297	Positron Emission Tomography Imaging of Vascular Endothelial Growth Factor Receptor Expression with ⁶¹ Cu-Labeled Lysine-Tagged VEGF ₁₂₁ . Molecular Pharmaceutics, 2012, 9, 3586-3594.	4.6	16
298	ImmunoPET Imaging of Insulin-Like Growth Factor 1 Receptor in a Subcutaneous Mouse Model of Pancreatic Cancer. Molecular Pharmaceutics, 2016, 13, 1958-1966.	4.6	16
299	Surfactant-Stripped Pheophytin Micelles for Multimodal Tumor Imaging and Photodynamic Therapy. ACS Applied Bio Materials, 2019, 2, 544-554.	4.6	16
300	Catalytic radiosensitization: Insights from materials physicochemistry. Materials Today, 2022, 57, 262-278.	14.2	16
301	Imaging Gene Expression in Live Cells and Tissues. Cold Spring Harbor Protocols, 2011, 2011, pdb.top103.	0.3	15
302	ImmunoPET Imaging of CD146 in Murine Models of Intrapulmonary Metastasis of Non-Small Cell Lung Cancer. Molecular Pharmaceutics, 2017, 14, 3239-3247.	4.6	15
303	A Switchable Site-Specific Antibody Conjugate. ACS Chemical Biology, 2018, 13, 958-964.	3.4	15
304	Development and characterization of CD54-targeted immunoPET imaging in solid tumors. European Journal of Nuclear Medicine and Molecular Imaging, 2020, 47, 2765-2775.	6.4	15
305	ImmunoPET/NIRF/Cerenkov multimodality imaging of ICAM-1 in pancreatic ductal adenocarcinoma. European Journal of Nuclear Medicine and Molecular Imaging, 2021, 48, 2737-2748.	6.4	14
306	Molecular imaging of insulin-like growth factor 1 receptor in cancer. American Journal of Nuclear Medicine and Molecular Imaging, 2012, 2, 248-259.	1.0	14

#	Article	IF	CITATIONS
307	Targeted Cancer Therapy with Tumor Necrosis Factor-Alpha. Biochemistry Insights, 2008, 2008, 15-21.	3.3	14
308	Positron emission tomography imaging of CD105 expression in a rat myocardial infarction model with (64)Cu-NOTA-TRC105. American Journal of Nuclear Medicine and Molecular Imaging, 2013, 4, 1-9.	1.0	14
309	Facile and efficient assembly of collagen-like triple helices on a TRIS scaffold. Bioorganic Chemistry, 2007, 35, 327-337.	4.1	13
310	Dynamic PET imaging with ultra-low-activity of 18F-FDG: unleashing the potential of total-body PET. European Journal of Nuclear Medicine and Molecular Imaging, 2021, 48, 4138-4141.	6.4	13
311	ImmunoPET of CD146 in Orthotopic and Metastatic Breast Cancer Models. Bioconjugate Chemistry, 2021, 32, 1306-1314.	3.6	13
312	Antioxidant and C5a-blocking strategy for hepatic ischemia–reperfusion injury repair. Journal of Nanobiotechnology, 2021, 19, 107.	9.1	13
313	Coordination chemistry of [Y(pypa)] ^{â^'} and comparison immuno-PET imaging of [⁴⁴ Sc]Sc- and [⁸⁶ Y]Y-pypa-phenyl-TRC105. Dalton Transactions, 2020, 49, 5547-5562.	3.3	12
314	ImmunoPET Imaging of TIMâ€3 in Murine Melanoma Models. Advanced Therapeutics, 2020, 3, 2000018.	3.2	12
315	64Cu-labeled daratumumab F(ab′)2 fragment enables early visualization of CD38-positive lymphoma. European Journal of Nuclear Medicine and Molecular Imaging, 2022, 49, 1470-1481.	6.4	12
316	Novel Small Molecule Probes for Metastatic Melanoma. ACS Medicinal Chemistry Letters, 2017, 8, 179-184.	2.8	11
317	Selfâ€Amplified Photodynamic Therapy through the ¹ O ₂ â€Mediated Internalization of Photosensitizers from a Ppaâ€Bearing Block Copolymer. Angewandte Chemie, 2020, 132, 3740-3746.	2.0	11
318	First clinical experience of 106Âcm, long axial field-of-view (LAFOV) PET/CT: an elegant balance between standard axial (23Âcm) and total-body (194Âcm) systems. European Journal of Nuclear Medicine and Molecular Imaging, 2021, 48, 3755-3759.	6.4	11
319	Pravastatin stimulates angiogenesis in a murine hindlimb ischemia model: a positron emission tomography imaging study with (64)Cu-NOTA-TRC105. American Journal of Translational Research (discontinued), 2013, 6, 54-63.	0.0	11
320	Dual-labeled pertuzumab for multimodality image-guided ovarian tumor resection. American Journal of Cancer Research, 2019, 9, 1454-1468.	1.4	11
321	PET imaging of macrophages in cardiovascular diseases. American Journal of Translational Research (discontinued), 2020, 12, 1491-1514.	0.0	11
322	The new science of protein mimetics. Macromolecular Symposia, 2003, 201, 223-236.	0.7	10
323	Efficient Uptake of ¹⁷⁷ Luâ€Porphyrinâ€PEG Nanocomplexes by Tumor Mitochondria for Multimodalâ€Imagingâ€Guided Combination Therapy. Angewandte Chemie, 2018, 130, 224-228.	2.0	10
324	Engineering biocompatible TeSex nano-alloys as a versatile theranostic nanoplatform. National Science Review, 2021, 8, .	9.5	10

#	Article	IF	CITATIONS
325	Endoglin/CD105-Based Imaging of Cancer and Cardiovascular Diseases: A Systematic Review. International Journal of Molecular Sciences, 2021, 22, 4804.	4.1	10
326	HER2-targeted multimodal imaging of anaplastic thyroid cancer. American Journal of Cancer Research, 2019, 9, 2413-2427.	1.4	10
327	Harnessing DNA for Immunotherapy: Cancer, Infectious Diseases, and Beyond. Advanced Functional Materials, 2022, 32, .	14.9	10
328	Harnessing the Power of Molecular Imaging for Precision Medicine. Journal of Nuclear Medicine, 2016, 57, 171-172.	5.0	9
329	Cancer theranostics with 64Cu/177Lu-loaded liposomes. European Journal of Nuclear Medicine and Molecular Imaging, 2016, 43, 938-940.	6.4	9
330	Chelatorâ€Free Radiolabeling of Nanographene: Breaking the Stereotype of Chelation. Angewandte Chemie, 2017, 129, 2935-2938.	2.0	9
331	The bold legacy of Emil Fischer. Journal of Peptide Science, 2003, 9, 594-603.	1.4	8
332	Smaller Agents for Larger Therapeutic Indices: Nanoscale Brachytherapy with ¹⁷⁷ Lu-Labeled Gold Nanoparticles. Journal of Nuclear Medicine, 2016, 57, 834-835.	5.0	8
333	The new era of cancer immunotherapy: what can molecular imaging do to help?. Clinical and Translational Imaging, 2017, 5, 299-301.	2.1	8
334	Multimodale Kontrastmittel für die kombinierte Positronenemissionstomographie. Angewandte Chemie, 2019, 131, 2592-2602.	2.0	8
335	First-in-human study of an 18F-labeled boramino acid: a new class of PET tracers. European Journal of Nuclear Medicine and Molecular Imaging, 2021, 48, 3037-3040.	6.4	8
336	Molecular MRI of VEGFR-2 reveals intra-tumor and inter-tumor heterogeneity. American Journal of Nuclear Medicine and Molecular Imaging, 2013, 3, 312-6.	1.0	8
337	ImmunoPET imaging of CD38 expression in hepatocellular carcinoma using Cu-labeled daratumumab. American Journal of Translational Research (discontinued), 2019, 11, 6007-6015.	0.0	8
338	Engineering CpGâ€ASOâ€Ptâ€Loaded Macrophages (CAP@M) for Synergistic Chemo″Gene″Immunoâ€Thera Advanced Healthcare Materials, 2022, 11, .	^{ру} .6	8
339	Generation and Screening of Monoclonal Antibodies for ImmunoPET Imaging of IGF1R in Prostate Cancer. Molecular Pharmaceutics, 2014, 11, 3624-3630.	4.6	7
340	ImmunoPET of CD146 in a Murine Hindlimb Ischemia Model. Molecular Pharmaceutics, 2018, 15, 3434-3441.	4.6	7
341	Nanoparticles as Radiopharmaceutical Vectors. , 2019, , 181-203.		7
342	Total-Body PET Imaging for up to 30 Days After Injection of ⁸⁹ Zr-Labeled Antibodies. Journal of Nuclear Medicine, 2020, 61, 451-452.	5.0	7

#	Article	IF	CITATIONS
343	Immuno-PET imaging of VEGFR-2 expression in prostate cancer with Zr-labeled ramucirumab. American Journal of Cancer Research, 2019, 9, 2037-2046.	1.4	7
344	Enhancing fibroblast activation protein (FAP)-targeted radionuclide therapy with albumin binding, and beyond. European Journal of Nuclear Medicine and Molecular Imaging, 2022, , 1.	6.4	7
345	Auger electron-based targeted radioimmunotherapy with 58mCo, a feasibility study. AIP Conference Proceedings, 2016, , .	0.4	6
346	Radio-nanomaterials for biomedical applications: state of the art. European Journal of Nanomedicine, 2016, 8, 151-170.	0.6	6
347	Next-Generation Molecular Imaging of Thyroid Cancer. Cancers, 2021, 13, 3188.	3.7	6
348	Head-to-Head Comparison of Neck 18F-FDG PET/MR and PET/CT in the Diagnosis of Differentiated Thyroid Carcinoma Patients after Comprehensive Treatment. Cancers, 2021, 13, 3436.	3.7	6
349	PET with a ⁶⁸ Ga-Labeled FAPI Dimer: Moving Toward Theranostics. Journal of Nuclear Medicine, 2022, 63, 860-861.	5.0	6
350	HaloTag as a reporter gene: positron emission tomography imaging with (64)Cu-labeled second generation HaloTag ligands. American Journal of Translational Research (discontinued), 2013, 5, 291-302.	0.0	6
351	Imaging the Biodistribution and Performance of Transplanted Stem Cells with PET. Journal of Nuclear Medicine, 2016, 57, 1331-1332.	5.0	5
352	Radionuklidaktivierte Nanomaterialien und ihre biomedizinische Anwendung. Angewandte Chemie, 2019, 131, 13366-13387.	2.0	5
353	Spatiotemporal Distribution of Agrin after Intrathecal Injection and Its Protective Role in Cerebral Ischemia/Reperfusion Injury. Advanced Science, 2020, 7, 1902600.	11.2	5
354	Engineering of Mesoporous Silica Nanoparticles for In Vivo Cancer Imaging and Therapy. , 2014, , 611-640.		4
355	Positron Emission Tomography: State of the Art. Molecular Pharmaceutics, 2014, 11, 3773-3776.	4.6	4
356	64Cu-Labeled Aptamers for Tumor-Targeted Radionuclide Delivery. Methods in Molecular Biology, 2019, 1974, 223-231.	0.9	4
357	Intrinsically Zr-labeled GdOS:Eu nanophosphors with high stability for dual-modality imaging. American Journal of Translational Research (discontinued), 2016, 8, 5591-5600.	0.0	4
358	ImmunoPET of CD38 with a radiolabeled nanobody: promising for clinical translation. European Journal of Nuclear Medicine and Molecular Imaging, 2021, 48, 2683-2686.	6.4	3
359	Engineering Carbon Nanomaterials for Stem Cell-Based Tissue Engineering. , 2014, , 641-665.		3
360	Dimeric FAPI with potential for tumor theranostics American Journal of Nuclear Medicine and Molecular Imaging, 2021, 11, 537-541.	1.0	3

#	Article	IF	CITATIONS
361	Scaffold Assembly of Collagen-Like Triple Helices at the C-Terminus. Letters in Organic Chemistry, 2007, 4, 96-101.	0.5	2
362	Cancer Theranostics with Carbon-Based Nanoplatforms. , 2014, , 347-361.		2
363	One-step synthesis of an 18F-labeled boron-derived methionine analog: a substitute for 11C-methionine?. European Journal of Nuclear Medicine and Molecular Imaging, 2018, 45, 582-584.	6.4	2
364	Exogenous Radionanomedicine: Inorganic Nanomaterials. Biological and Medical Physics Series, 2018, , 13-47.	0.4	2
365	Imaging and therapy of diabetes: State of the art. Advanced Drug Delivery Reviews, 2019, 139, 1-2.	13.7	2
366	Labeling of Erythrocytes by Porphyrinâ€Phospholipid. Advanced NanoBiomed Research, 2021, 1, 2000013.	3.6	2
367	New wine in old bottles: Ga-PSMA-11 PET/CT reveals COVID-19 in patients with prostate cancer. American Journal of Nuclear Medicine and Molecular Imaging, 2021, 11, 332-336.	1.0	2
368	Molecular Imaging: Intrinsically Radiolabeled Nanoparticles: An Emerging Paradigm (Small 19/2014). Small, 2014, 10, 3824-3824.	10.0	1
369	In Vivo Imaging of Inflammation and Infection. Contrast Media and Molecular Imaging, 2018, 2018, 1-2.	0.8	1
370	Predicting PD-1/PD-L1 status in bladder cancer with 18F-FDG PET?. European Journal of Nuclear Medicine and Molecular Imaging, 2019, 46, 791-793.	6.4	1
371	Frontispiece: Chiralityâ€Driven Transportation and Oxidation Prevention by Chiral Selenium Nanoparticles. Angewandte Chemie - International Edition, 2020, 59, .	13.8	1
372	Engineering Upconversion Nanoparticles for Biomedical Imaging and Therapy. , 2014, , 585-609.		1
373	Multimodality imaging of <scp>nanoparticleâ€based</scp> vaccines: Shedding light on immunology. Wiley Interdisciplinary Reviews: Nanomedicine and Nanobiotechnology, 2022, , e1807.	6.1	1
374	State-of-the-art of nuclear medicine and molecular imaging in China: after the first 66Âyears (1956–2022). European Journal of Nuclear Medicine and Molecular Imaging, 2022, 49, 2455-2461.	6.4	1
375	The New Science of Protein Mimetics. ChemInform, 2004, 35, no.	0.0	0
376	Scaffold, Dendritic and Metal-Assisted Assembly of Collagen-Like Biomaterials. , 2006, , 42-43.		0
377	Fluorescent Dye Conjugates for Optical Imaging of Cancer. , 2012, , 451-482.		0
378	Integrin αvβ3-Targeted Optical Imaging with Metal Oxide Nanomaterials: Focusing on Zinc Oxide. Methods in Pharmacology and Toxicology, 2015, , 123-134.	0.2	0

#	Article	IF	CITATIONS
379	Highlights from the latest articles in nanomedicine for deep tumor imaging and phototherapy. Nanomedicine, 2015, 10, 1681-1683.	3.3	0
380	Development and characterization of a hexamodal imaging nanoparticle. , 2015, , .		0
381	Multimodal Imaging: Surfactant‣tripped Frozen Pheophytin Micelles for Multimodal Gut Imaging (Adv.) Tj ETQ	q1_1.0.784 21.0	4314 rgBT /0
382	Theranostic Nanoplatforms for PET Image-Guided Drug Delivery. , 2017, , 257-275.		0
383	Frontispiz: Chiralityâ€Driven Transportation and Oxidation Prevention by Chiral Selenium Nanoparticles. Angewandte Chemie, 2020, 132, .	2.0	0
384	High-performance renal imaging with a radiolabeled, non-excretable chimeric fusion protein. Theranostics, 2021, 11, 9177-9179.	10.0	0
385	Chapter 16. Recent Advances in The Engineering of Silica-Based Core@Shell Structured Hybrid Nanoparticles. , 2016, , 415-438.		0
386	ImmunoPET of the differential expression of CD146 in breast cancer. American Journal of Cancer Research, 2021, 11, 1586-1599.	1.4	0